

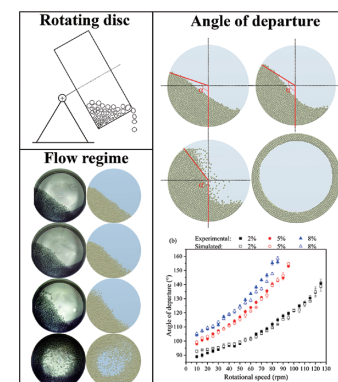
Effects of DEM Parameters and Operating Conditions on Particle Dynamics in a Laboratory Scale Rotating Disc[†]

Rondinelli M. Lima, Gisele M. Souza, Rodolfo J. Brandão, Claudio R. Duarte and Marcos A.S. Barrozo*

School of Chemical Engineering, Federal University of Uberlândia, Brazil

Rotating discs are usually used as granulators in many industrial processes. The efficiency of the granulation process in this device is directly related to the particle motion behavior in different flow regimes. In this work, the granular flow in a rotating disc was investigated experimentally and numerically. The Discrete Element Method (DEM) was used in the simulations, while Central Composite Designs (CCD) were employed to quantify the effects of DEM input parameters and operating conditions (filling degree (FD), angle of inclination (AI), and rotational speed) on the contacts between particles. The results showed that the particle–wall static friction coefficient had the most significant impact on the studied response. Additionally, the effect of operating variables on the collision force between particles, the angle of departure and particle velocities were successfully investigated, with corresponding DEM simulation predictions. It was also verified that the simulations performed with experimentally measured DEM input parameter values were able to reproduce the flow regimes in the rotating disc.

Keywords: rotating disc, flow regimes, DEM, DEM parameters, number of contacts



1. Introduction

The granulation process is widely employed in different industries, such as fertilizer, pharmaceutical, food, chemical, steel, and ceramics. This particle size enlargement technique allows the production of useful structural forms, modifies the material rheology, increases its flowability, reduces material loss and dust emissions, and controls porosity (Capes, 1980; Litster and Ennis, 2004).

Industrial granulators promote agglomeration through particle mixing and collision. Compared to other types of equipment, rotating discs stand out due to their pronounced segregation ability and flexibility to operate different types of materials (Litster and Ennis, 2004). Moreover, their geometry is relatively simple, consisting of a disc with a certain diameter (D), an angle of inclination (θ) and a rim (L) that rotates around its axis (Fig. 1).

Although rotating discs have been widely used as a granulator (Azrar et al., 2016; Ball, 1959; Chadwick and Bridgwater, 1997), only qualitative descriptions of solids flow have been usually made, with little quantitative information on particle dynamics (Chadwick and Bridgwater, 1997). The effects of different operating variables, such as rotational speed, filling degree (FD) and angle of inclina-

tion (AI), on the motion and contacts of particles are still not fully understood (Lima et al., 2022). Furthermore, as granulation is a dynamic process, investigating both the responses that are directly related to the granule formation (i.e., particle velocity, and number and force of contacts between particles) and flow regimes can also be a potential tool to optimize the granulation process in rotating discs (Gladky et al., 2021).

Depending on the operating conditions, different regimes of solids motion can be identified in a rotating disc: slipping, rolling, cascading, cataracting, and centrifuging, each with a specific flow behavior. Detailed descriptions of these flow regimes can be found in Mellmann (2001).

In the rolling regime, the granular bed can be divided into two distinct regions: the passive layer, where the particles are dragged up by the disc wall as a rigid body, and the active layer, where the particles roll over the bed surface downwards. For higher velocities, a kidney-shaped curve develops on the bed surface and a larger area of the disc is used, corresponding to the cascading regime. Regarding the granulation process, the rolling and cascading regimes in particular have the advantage of promoting more effective contacts between particles than the others (Azrar et al., 2016; Salman et al., 2006).

In addition to experimental studies, numerical simulations have become a complementary tool in granular flow analysis. Introduced by Cundall and Strack (1979), the Discrete Element Method (DEM) has been extensively applied to investigate granular dynamics in different types of equipment. In this method, each particle is described

[†] Received 30 March 2023; Accepted 1 May 2023
J-STAGE Advance published online 31 August 2023

* Corresponding author: Marcos A.S. Barrozo;
Add: Bloco K, Campus Santa Mônica, 38400-902, Uberlândia, MG, Brazil
E-mail: masbarrozo@ufu.br
FAX: +55-34-32394188

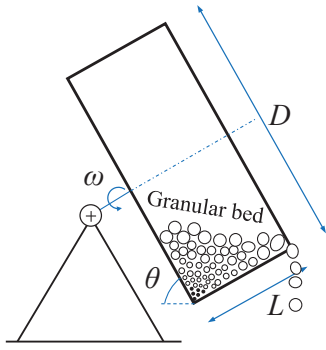


Fig. 1 Schematic diagram of a rotating disc.

individually through the application of a balance of forces and contact laws. The precision of the DEM model for predicting the granular flow relies on the selected contact model and the input parameters, which depend on both the particle properties and the particle-contact properties.

DEM simulations provide microscopic results at the particle level, such as trajectories of particles and forces that act on them, making it possible to obtain important information about particle dynamics. In this context, the knowledge of the solids flow in rotating discs is crucial for their design and applicability. However, there are a limited number of studies on the fluid dynamics of rotating discs using numerical analysis in conjunction with experimental results. Thus, through the use of DEM simulations and experimental data the present work aims to investigate how numerical parameters and different operating conditions influence particle dynamics in a rotating disc. The flow regimes and particle velocity distributions were also studied.

2. Discrete element method

DEM uses a time-stepping algorithm where the modeling is repeated in each time interval. Each particle is tracked contact by contact and its positions are updated based on the results of the previous time step (Nascimento et al., 2022; O’Sullivan, 2011). During each time step, Newton’s second law is applied to determine the particle trajectory, while the particle–particle and particle–wall contact forces are evaluated based on the force–displacement law (Brandao et al., 2020; Cundall and Strack, 1979; Potyondy and Cundall, 2004). The motion of individual particles is determined by Eqns. (1) and (2):

$$m_i \frac{dv_i}{dt} = \sum_j F_{ij} \quad (1)$$

$$I_i \frac{d\omega_i}{dt} = \sum_j \tau_{ij} \quad (2)$$

where t , m_i , I_i , v_i , and ω_i are the time, mass, moment of inertia, linear velocity, and angular velocity of particle i , respectively, and F_{ij} and τ_{ij} are the force and torque between

Table 1 Nonlinear Hertz–Mindlin model equations (Cundall and Strack, 1979; Di Maio and Di Renzo, 2005; Tsuji et al., 1992).

Normal force	$F_n = \frac{4}{3} E^* \sqrt{R^*} \delta_n^{\frac{3}{2}}$	(3)
Damping normal force	$F_n^d = -2\sqrt{\frac{5}{6}} \beta \sqrt{S_n m^*} v_n^{\text{rel}}$	(4)
Equivalent contact radius	$\frac{1}{R^*} = \frac{1}{R_i} + \frac{1}{R_j}$	(5)
Equivalent mass	$\frac{1}{m^*} = \frac{1}{m_i} + \frac{1}{m_j}$	(6)
Equivalent Young’s modulus	$\frac{1}{E^*} = \frac{1-\nu_i^2}{E_i} + \frac{1-\nu_j^2}{E_j}$	(7)
Normal stiffness	$S_n = 2E^* \sqrt{R^*} \delta_n$	(8)
Damping coefficient	$\beta = \frac{\ln e}{\sqrt{\ln^2 e + \pi^2}}$	(9)
Tangential force	$F_t = -\delta_t S_t$	(10)
Tangential damping force	$F_t^d = -2\sqrt{\frac{5}{6}} \beta \sqrt{S_t m^*} v_t^{\text{rel}}$	(11)
Tangential stiffness	$S_t = 8G^* \sqrt{R^*} \delta_n$	(12)
Equivalent shear modulus	$\frac{1}{G^*} = \frac{2-\nu_i}{G_i} + \frac{2-\nu_j}{G_j}$	(13)

particles i and j , respectively.

The contact model used herein was the nonlinear Hertz–Mindlin. The main equations of this model are summarized in Table 1.

The equations in the Table 1 involve normal and tangential overlaps (δ_n , δ_t), normal and tangential relative velocities (v_n^{rel} , v_t^{rel}), restitution coefficient (e), and Poisson’s ratio (ν).

3. Materials and methods

Laboratory tests and numerical simulations were conducted using a disc granulator made of stainless steel with a smooth surface and diameter of 35 cm, length of 20 cm, and variable angle of inclination. The granular material used was glass beads with a diameter of 6.35 ± 0.01 mm, density of 2455 ± 24 kg/m³, and sphericity of 0.99 ± 0.01 .

The DEM simulations were performed on the commercial EDEM[®] software. To ensure the numerical stability of the simulation, a time step of 4×10^{-5} s, which is equivalent to 20 % of the Rayleigh time, was adopted. The simulation conditions are listed in Table 2.

3.1 Measurement of DEM input parameters

The restitution coefficient (e), which quantifies the energy conserved in shocks between solid bodies, can be experimentally measured by the ratio between the relative velocities after (V_1) and before (V_0) the impact of two colliding bodies (Lima et al., 2021; Machado et al., 2017; Marinack Jr. et al., 2013), as shown in Eqn. (14):

$$e = \frac{V_1}{V_0} \tag{14}$$

To determine the velocity before and after collision, the experimental apparatus described in previous studies was employed (Bharadwaj et al., 2010; Hastie, 2013; Marinack Jr. et al., 2013). It consists of a vacuum pump responsible for a suction pressure that holds particles at a height of 50 mm from the plate. In this procedure, the pump is switched off to allow particles to fall, while their trajectory is filmed by a high-speed video camera (Fastec IL5—up to 44,000 frames/s).

In order to measure the static friction coefficient (μ_s), the inclined plane method was applied (ASTM G115-10, 2013). In this method, the plane is gradually inclined and the angle of inclination (Φ) from which the particles start to slide is used to calculate the μ_s (Eqn. (15)).

$$\mu_s = \tan(\Phi) \tag{15}$$

To replicate the particle–wall interactions, the surface of the inclined plane was covered with a stainless steel plate. The particle–particle interaction behavior was studied by covering the surface of the plane with a fixed granular bed of glass beads (Brandao et al., 2020; Lima et al., 2021).

To calculate the rolling friction coefficient (μ_R), a measurement procedure based on that described in Lima et al. (2022) was adopted. The particle was placed on the top of

the launching device (Fig. 2) at a certain height (h_0), and then allowed to travel through the entire device. The distance traveled by the particle after leaving the launching device until its resting point (D_r) was subsequently measured. The rolling friction coefficient was calculated using Eqn. (16):

$$\mu_R = \frac{h_0}{D_r} \tag{16}$$

The experimental parameter values were used herein as inputs to the DEM model. Brandao et al. (2020) showed that the simulations performed with experimentally measured parameters were in good agreement with the experimental responses.

3.2 Sensitivity analysis of DEM parameters

In order to quantify the effect of DEM parameters (i.e., restitution, static, and rolling friction coefficients) on the contact between particles in the rotating disc, a fractional Central Composite Design (CCD) (2^{6-1} , with 2x6 axial points and one central point) was used for the DEM calibration procedure. The CCD levels are shown in Table 3.

The CCD data was used to better understand the influence of the DEM parameters on the rotating disc simulation. Therefore, the CCD can help in both the calibration process and the development of new disc designs.

This CCD was applied to angles of inclination of 40°, 50° and 60°, and the rotating disc was filled with glass beads (2 % per volume). The rotational speed was set at 10 rpm. The dependent variable (response) was the average number of contacts between particles ($N_{C_{pp}}$), since it is a relevant parameter in the granulation process. The greater the contact between particles, the more effective the granulation process.

For each CCD run, the real-time simulation was 30 s. The $N_{C_{pp}}$ average was obtained in the last 10s of simulation, since the rotating disc was operating in steady state. The steady-state condition was considered when the granular bed reached a constant height.

Table 2 DEM simulation conditions.

Model	Hertz–Mindlin
Time step (s)	4×10^{-5}
Poisson’s ratio (-)	
Glass beads	0.22
Stainless steel	0.30
Shear modulus (Pa)	
Glass beads	1×10^6
Stainless steel	7×10^{10}

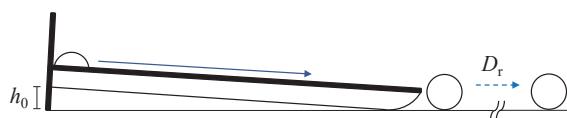


Fig. 2 Rolling friction coefficient apparatus.

Table 3 CCD levels used in the sensitivity analysis of DEM parameters.

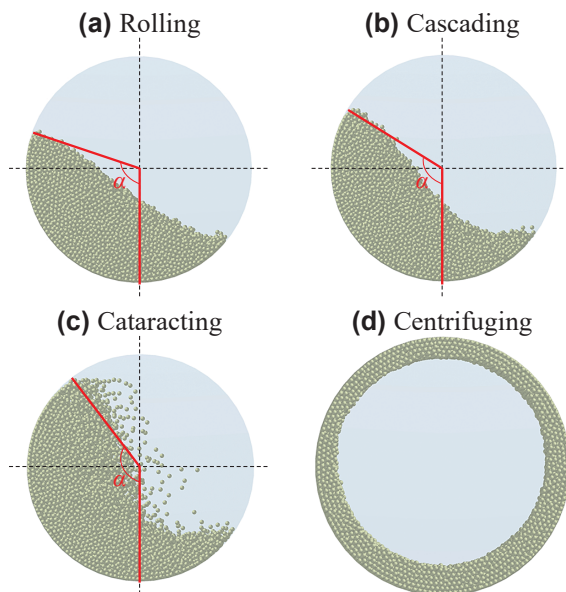
Factor coding	$e_{pp}, e_{pw}, \mu_{S_{pp}}, \mu_{S_{pw}}$	$\mu_{R_{pp}}, \mu_{R_{pw}}$
$-\alpha$ (-1.78)	0.054	0.005
-1	0.250	0.025
0	0.500	0.050
1	0.750	0.075
$+\alpha$ (+1.78)	0.946	0.095

* $e_{pp}, e_{pw}, \mu_{S_{pp}}, \mu_{S_{pw}}, \mu_{R_{pp}}, \mu_{R_{pw}}$ correspond to the restitution, static, and rolling friction coefficients, respectively. The subscripts pp and pw indicate the particle–particle and particle–wall interactions, respectively.

Table 4 CCD levels used in the sensitivity analysis of operating conditions.

Coded Factor	FD (%)	AI ($^{\circ}$)	RS (rpm)							
$-\alpha$ (-1.47)	0.59	35.29	5.29							
-1	2.00	40.00	10.00							
0	5.00	50.00 </tr <tr> <td>+1</td> <td>8.00</td> <td>60.00</td> <td>30.00</td> </tr> <tr> <td>$+\alpha$ (+1.47)</td> <td>9.41</td> <td>64.71</td> <td>34.71</td> </tr>	+1	8.00	60.00	30.00	$+\alpha$ (+1.47)	9.41	64.71	34.71
+1	8.00	60.00	30.00							
$+\alpha$ (+1.47)	9.41	64.71	34.71							

* FD : filling degree, AI : angle of inclination, RS : rotational speed.

**Fig. 3** Analyzed flow regimes and angle of departure measurement.

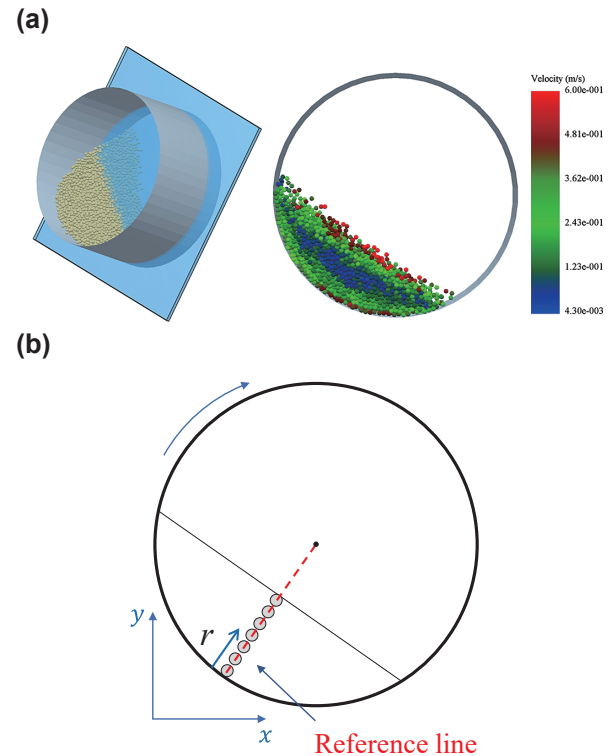
3.3 Sensitivity analysis of operating conditions

Another CCD was applied to evaluate the sensitivity of operating conditions on the number of contacts between particles. For these simulations the DEM parameters were kept constant following the values defined in Section 3.1. The analyzed operating conditions and the corresponding CCD levels are listed in Table 4.

3.4 Simulation of flow regimes

The flow regimes (i.e., rolling, cascading, cataracting, and centrifuging) were numerically investigated and compared with experimental results of our previous work (Lima et al., 2022). The angle of departure (α) was defined as the angle at which the particles detached from the equipment wall; it was measured using the Measure software (Fig. 3).

The analyses were carried out at filling degrees of 2 %, 5 % and 8 % and angles of inclination of 40°, 50° and 60°. The flow regimes were simulated using experimental values of DEM parameters.

**Fig. 4** Determination of particle velocity distribution: (a) cross-section representation parallel to the base of the rotating disc; and (b) schematic representation for particle velocity measurement.

3.5 Simulation of particle velocity distributions

In order to determine the passive and active layers of the rolling regime, the particle velocities were measured. Due to the inclination of the rotating disc, these layers were located in the inner part of the granular bed. Therefore, it was necessary to perform a cross-sectional cut parallel to the base of the rotating disc, as illustrated in Fig. 4(a).

The particle velocity was determined along the reference line drawn in the middle of the granular bed (Fig. 4(b)) under different conditions (Delele et al., 2016; Resende et al., 2017; Santos et al., 2013, 2015). The reference line was discretized and normalized at evenly distributed points, and at each point the velocity of five different particles was determined.

The conditions used to investigate the velocity profiles of glass beads in the rotating disc were filling degrees of 2 % and 5 %, angles of inclination of 50° and 60°, and rotational speeds of 10 rpm, 15 rpm and 20 rpm.

4. Results and discussions

4.1 Sensitivity analysis of DEM parameters

A CCD (see levels in Table 3) was employed to evaluate the influence of DEM parameters on the number of contacts between particles ($N_{C_{pp}}$) in a rotating disc. To this end, a total of 45 simulations were performed for the rotating disc operating at angles of inclination of 40°, 50°, and 60°, a filling degree of 2 %, and a rotational speed of 10 rpm.

The obtained results are depicted in **Appendix A** (Supplementary material: **Table A1**).

From these results, it was possible to quantify such effects for each angle of inclination by regression techniques. The prediction equations (**Eqns. (17)–(19)**) resulted in correlation coefficients (R^2) of 0.94, 0.95 and 0.95 for angles of inclination of 40°, 50° and 60°, respectively.

$$N_{C_{pp-40^\circ}} = 1.17 - 0.05x_1 + 0.05x_1^2 + 0.05x_2^2 - 0.09x_3 - 0.36x_4 + 0.16x_4^2 + 0.06x_5^2 + 0.05x_6^2 \tag{17}$$

$$N_{C_{pp-50^\circ}} = 1.18 - 0.05x_1 + 0.06x_1^2 + 0.06x_2^2 - 0.12x_3 + 0.06x_3^2 - 0.40x_4 + 0.17x_4^2 + 0.07x_5^2 + 0.06x_6^2 - 0.04x_1x_4 \tag{18}$$

$$N_{C_{pp-60^\circ}} = 1.19 - 0.05x_1 + 0.06x_1^2 + 0.06x_2^2 - 0.13x_3 + 0.06x_3^2 - 0.41x_4 + 0.18x_4^2 + 0.07x_5^2 + 0.06x_6^2 - 0.03x_1x_4 \tag{19}$$

The DEM parameters of these equations are presented in coded form as follows:

$$\begin{aligned} x_1 &= \frac{e_{pp} - 0.50}{0.25} & x_2 &= \frac{e_{pw} - 0.50}{0.25} \\ x_4 &= \frac{\mu_{Spw} - 0.50}{0.25} & x_3 &= \frac{\mu_{Spp} - 0.50}{0.25} \\ x_5 &= \frac{\mu_{Rpp} - 0.050}{0.025} & x_6 &= \frac{\mu_{Rpw} - 0.050}{0.025} \end{aligned}$$

where x_1 = particle–particle restitution coefficient, x_2 = particle–wall restitution coefficient, x_3 = particle–particle static friction coefficient, x_4 = particle–wall static friction coefficient, x_5 = particle–particle rolling friction coefficient, and x_6 = particle–wall rolling friction coefficient, all in coded form.

In **Eqns. (17)–(19)**, only the statistically significant parameters were included. It was possible to observe that all DEM parameters had a significant effect on $N_{C_{pp}}$ at a significance level of 5 %.

The coefficients of **Eqns. (17)–(19)** show that e_{pw} (x_2 in coded form), μ_{Rpp} (x_5 in coded form), and μ_{Rpw} (x_6 in coded form) were only influenced by the quadratic term. On the other hand, μ_{Spw} (x_4 in coded form) was the parameter that most influenced $N_{C_{pp}}$, with an effect four times greater than that of μ_{Spp} (x_3 in coded form)—the second most relevant parameter—and eight times greater than that of e_{pp} (x_1 in coded form). In addition, the change in the angle of inclination of the rotating disc practically did not influence the intensity of the parameter effects.

In order to obtain accurate simulations based on the DEM approach, a correct set of input parameter values is required. Several studies have used the calibration process

to determine such values (Cunha et al., 2016; El Kassem et al., 2021; Marigo and Stitt, 2015; Nascimento et al., 2022; Santos et al., 2016). One of the disadvantages of the calibration process is the high number of simulations required to find the parameter values. Therefore, the analysis of the effects of DEM parameters becomes essential to quantify the influence of each parameter on the rotating disc. As μ_{Spw} has a much greater influence than the other parameters, an alternative is to only calibrate this parameter, thus reducing the number of simulations.

Another factor to be analyzed is that μ_{Spw} has a negative effect, i.e., the number of contacts between particles decreases as the coefficient value increases. This information is necessary for the design and optimization of rotating discs, because depending on the interaction between the granular material and the equipment wall, the contact between particles can decrease, thus hindering the granulation process.

Rong et al. (2020) used a 3^k factorial design to evaluate the sensitivity of particle–particle DEM parameters in a rotating drum. The authors found that the sliding friction coefficient, when compared with the rolling friction coefficient and the restitution coefficient, was the determining parameter on the mean power draw of the rotating drum. With the increase in the sliding friction coefficient, more power was required due to the increased resistance of particles when they come into contact with other particles.

Table 5 CCD used to analyze the influence of operating conditions on $N_{C_{pp}}$.

Run	FD (%)	AI (°)	RS (rpm)	$N_{C_{pp}}$
1	2.00	40.00	10.00	1.31
2	2.00	40.00	30.00	0.79
3	2.00	60.00	10.00	1.34
4	2.00	60.00	30.00	0.86
5	8.00	40.00	10.00	1.59
6	8.00	40.00	30.00	1.15
7	8.00	60.00	10.00	1.65
8	8.00	60.00	30.00	1.26
9	0.59	50.00	20.00	0.71
10	9.41	50.00	20.00	1.42
11	5.00	35.29	20.00	1.19
12	5.00	64.71	20.00	1.28
13	5.00	50.00	5.29	1.73
14	5.00	50.00	34.71	1.03
15	5.00	50.00	20.00	1.29

4.2 Analysis of the effects of operating conditions

Table 5 shows the results of the CCD used to analyze the influence of filling degree (*FD*), angle of inclination (*AI*) and rotational speed (*RS*) on $N_{C_{pp}}$ (see levels in **Table 4**).

The data in **Table 5** were subjected to regression analysis to quantify the effects of each independent variable and its corresponding interactions on the response ($N_{C_{pp}}$). The variables *FD*, *AI* and *RS* were coded as x_7 , x_8 , and x_9 , respectively. The obtained equation (**Eqn. (20)**) has a correlation coefficient (R^2) equal to 0.97.

$$N_{C_{pp}} = 1.27 + 0.19x_7 - 0.09x_7^2 + 0.03x_8 - 0.23x_9 + 0.06x_9^2 \quad (20)$$

$$\text{where: } x_7 = \frac{FD - 5\%}{3\%}; \quad x_8 = \frac{AI - 50^\circ}{10^\circ};$$

$$\text{and } x_9 = \frac{RS - 20\text{rpm}}{10\text{rpm}}$$

All operating conditions analyzed had a significant effect on $N_{C_{pp}}$ at a significance level of 5 %. It is noteworthy that there was no interaction between the variables, i.e., each variable alone had a direct influence on $N_{C_{pp}}$.

As it can be seen in **Eqn. (20)**, the effect of *FD* was positive, that is, the number of contacts between particles increased as a function of the number of particles in the rotating disc. An opposite effect was observed for rotational speed, i.e., the *RS* increased with decreasing $N_{C_{pp}}$. According to Capes (1980), during the granulation process the particle residence time can be lengthened by increasing the rotational speed. However, at high rotational speeds the rotating disc tends to operate in the cataracting regime, which can result in agglomerate degradation and breakage depending on the agitation intensity. A strict control of the rotational speed is then necessary for the rotating disc to operate in the rolling and cascading regimes, consequently improving the efficiency of the granulation process (Pietsch, 1997; Salman et al., 2006).

The change in the disc inclination had little influence on $N_{C_{pp}}$ when compared to the other variables. This result confirms what was observed in the sensitivity analysis of DEM parameters.

Other variables such as size distribution of feed, liquid content in the feed powder, and liquid surface tension can

also influence the granulation process (Capes, 1980). Nevertheless, **Eqn. (20)** can elucidate the granulation process, assisting in the operation, design and optimization of rotating discs.

4.3 Simulation of flow regimes

DEM simulations were also used to predict the behavior of flow regimes in a rotating disc. In these simulations, the input parameters obtained from the experimental procedure described in **Section 3.1** were employed. **Table 6** shows the values of DEM parameters obtained by the respective experimental measurement. To verify the validity of these DEM input parameters, the numerical and experimental results were compared. Two analyses were carried out: a qualitative one, where images of the flow regimes were confronted, and a quantitative one, where the angle of departure values were compared.

Figs. 5 to 7 compare the images of the experimental and simulated results for the different flow regimes in the rotating disc, operating at different angles of inclination (*AI*). As it can be seen, the DEM simulations accurately predicted each flow regime.

Regarding the quantitative analysis, **Fig. 8** compares the numerical and experimental angles of departure for the studied disc inclinations. As observed, the experimental and simulated results were very similar for the entire range of flow regimes (i.e., rolling, cascading, cataracting, and centrifuging). The average percentage deviation of the angle of departure was less than 2 %. Therefore, both qualitative (**Figs. 5 to 7**) and quantitative (**Fig. 8**) analyses confirmed that the direct experimental measurements of the DEM input parameters were able to reproduce the bulk behavior of particles in the rotating disc. For this reason, it was not necessary to perform the calibration of DEM parameters, allowing the preservation of their physical meanings.

Barrios et al. (2013) verified that experimental measurements of DEM parameters for a single particle proved to be a viable alternative to estimate the parameter values of iron ore pellets. According to the authors, the computational effort is reduced since the parameter values are obtained directly, without requiring a calibration process.

Brandao et al. (2020) used DEM Simulations to study the mixing and segregation of materials in a rotating drum. The authors measured the DEM parameters experimentally and performed a calibration approach. They verified that the parameter values obtained by the calibration process were similar to the experimental ones.

From the validation of the DEM model it can be verified that the DEM parameters successfully represent the evaluated experimental results. Therefore, it is possible to analyze the influence of the experimental operating conditions on the maximum collision force ($F_{C,max}$). To determine the maximum collision force, all particles were tracked along

Table 6 DEM parameter values obtained experimentally.

DEM parameters	Values
e_{pp}	0.900
e_{pw}	0.690
μ_{Spp}	0.620
μ_{Spw}	0.330
μ_{Rpp}	0.014
μ_{Rpw}	0.013

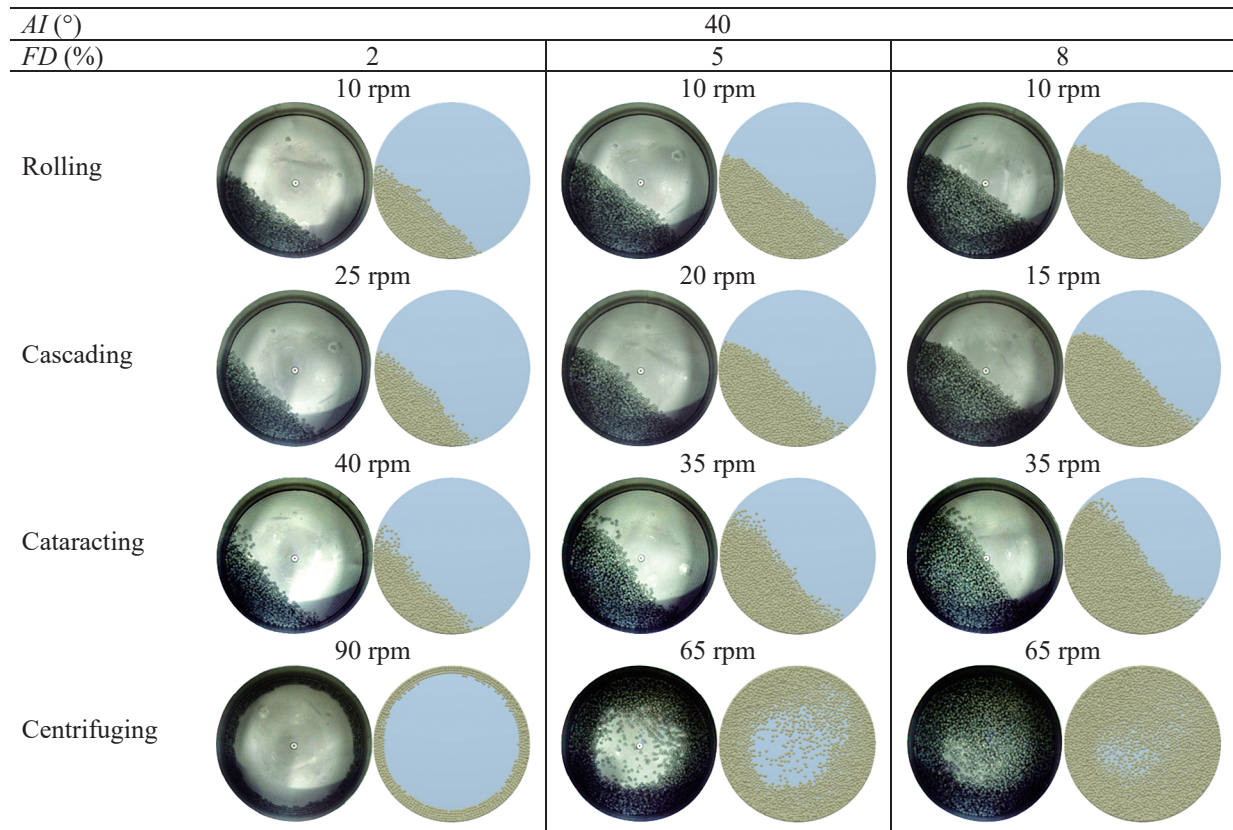


Fig. 5 Experimental and numerical results of the qualitative analysis of flow regimes for an angle of inclination of 40° .

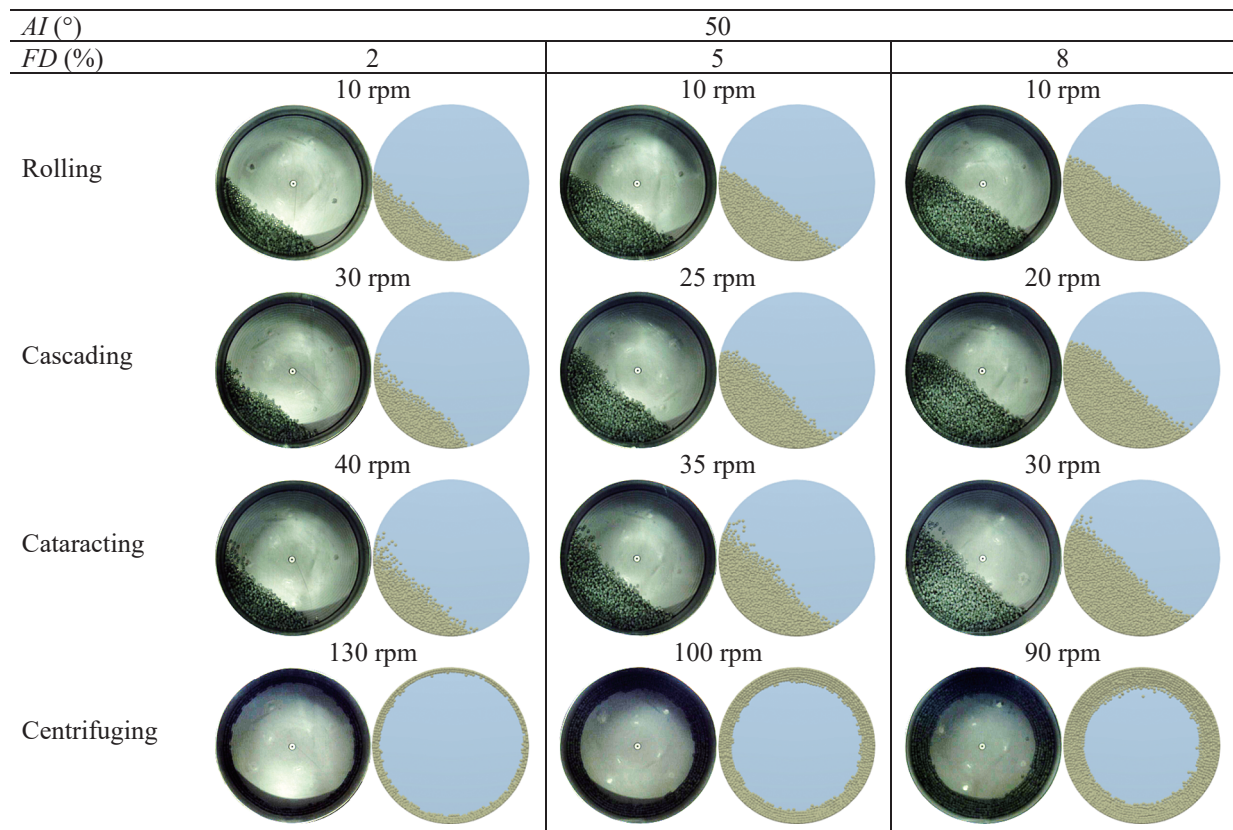


Fig. 6 Experimental and numerical results of the qualitative analysis of flow regimes for an angle of inclination of 50° .

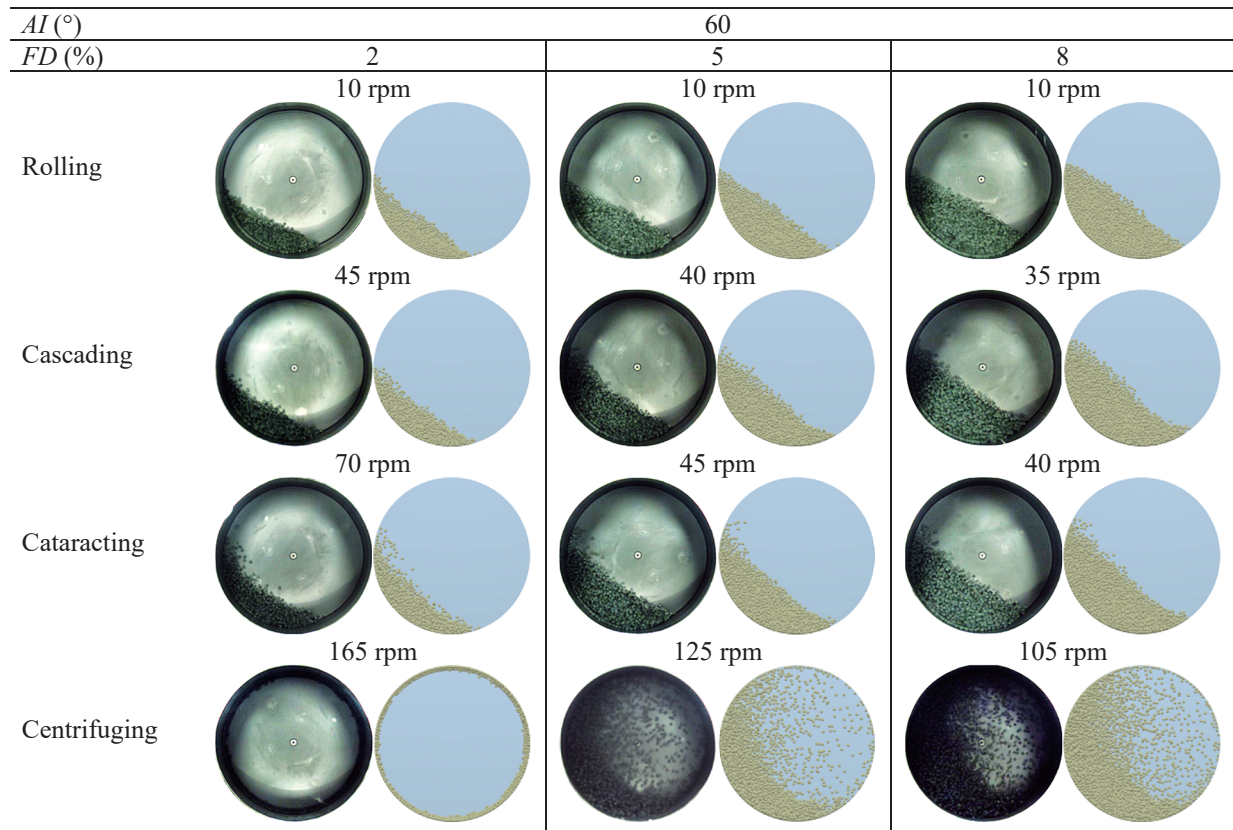


Fig. 7 Experimental and numerical results of the qualitative analysis of flow regimes for an angle of inclination of 60° .

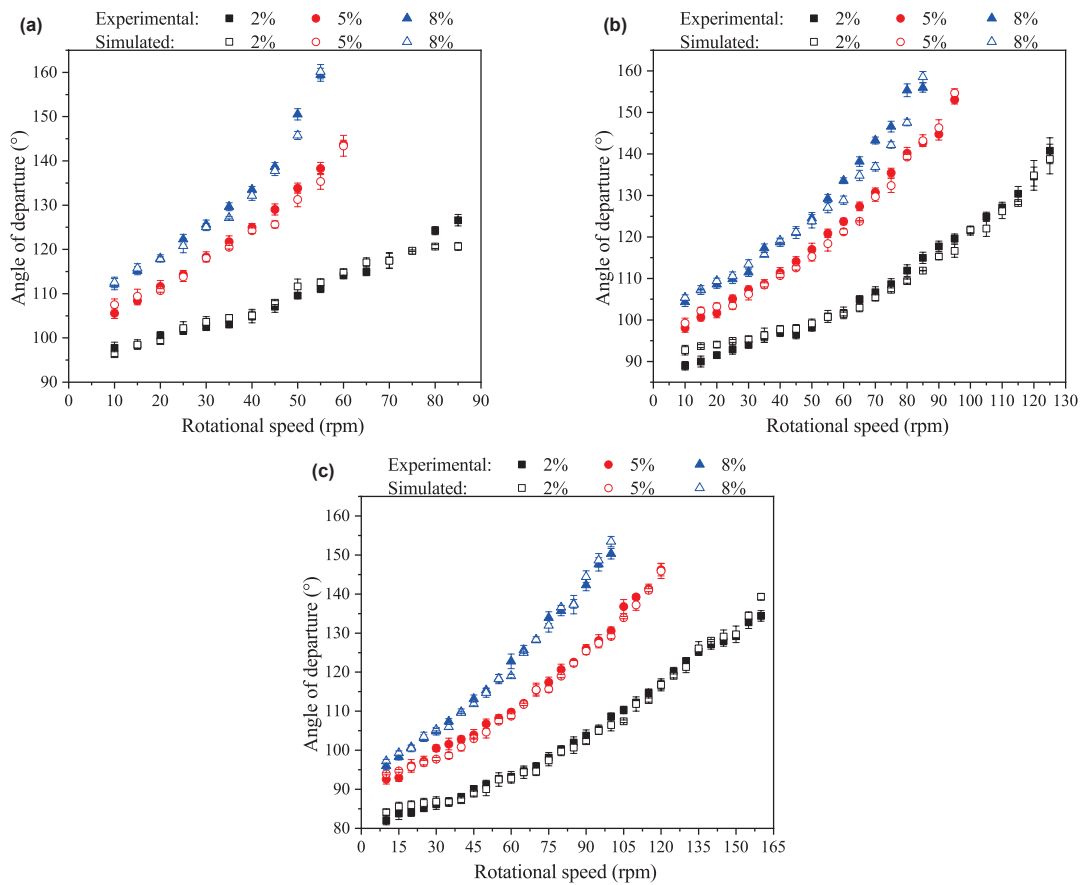


Fig. 8 Experimental and numerical results of the quantitative analysis of angles of departure for angles of inclination of (a) 40° , (b) 50° and (c) 60° .

the simulation time.

A 3^k factorial design was used to evaluate the effects of the following operating conditions on $F_{C,max}$: filling degree (FD), angle of inclination (AI) and rotational speed (RS). The levels used for the independent variables (FD , AI , and RS) were the same as the experimental ones. This analysis can be used to help prevent agglomerate degradation and breakage.

Table 7 shows the conditions and results ($F_{C,max}$) of the 3^k factorial design.

The effects of FD , AI and RS on $F_{C,max}$ were quantified by regression techniques using the experimental data in **Table 7**. From **Eqn. (21)**, which has a correlation coefficient (R^2) equal to 0.82, it is possible to predict the maxi-

Table 7 3^k factorial design used to analyze the influence of operating conditions of a rotating disc on $F_{C,max}$.

Run	FD (%)	AI (°)	RS (rpm)	$F_{C,max}$ (N)
1	2	40	10	1.10
2	2	40	30	1.52
3	2	40	50	1.98
4	2	50	10	1.21
5	2	50	30	1.33
6	2	50	50	1.62
7	2	60	10	1.18
8	2	60	30	1.72
9	2	60	50	1.93
10	5	40	10	1.24
11	5	40	30	1.46
12	5	40	50	2.31
13	5	50	10	1.21
14	5	50	30	1.43
15	5	50	50	1.80
16	5	60	10	1.45
17	5	60	30	1.91
18	5	60	50	1.72
19	8	40	10	1.35
20	8	40	30	1.74
21	8	40	50	2.91
22	8	50	10	1.55
23	8	50	30	1.49
24	8	50	50	1.68
25	8	60	10	1.52
26	8	60	30	1.50
27	8	60	50	1.75

imum collision force between particles ($F_{C,max}$) as a function of the operational variables and quantify its respective effects. The independent variables FD , AI , and RS are presented in coded forms (x_{10} , x_{11} and x_{12} , respectively).

All operating conditions had a positive effect on $F_{C,max}$ at a significance level of 5 %. $F_{C,max}$ increased as a function of both FD (x_{10} in coded form) and RS (x_{12} in coded form), with the latter affecting this variable three times more than the former. This analysis highlights the care that must be taken when operating rotating discs at high rotational speeds, as this can result in degradation of the agglomerates formed, thus impairing the granulation process. On the other hand, AI (x_{11} in coded form) had a negative effect on $F_{C,max}$, and although it did not affect linearly the collision force, it interacted with other variables.

$$F_{C,max} = 1.61 + 0.10x_{10} - 0.10x_{11}^2 + 0.33x_{12} - 0.12x_{10}x_{11} - 0.19x_{11}x_{12} + 0.09x_{11}x_{12}^2 - 0.10x_{11}^2x_{12} \quad (21)$$

where: $x_{10} = \frac{FD - 5\%}{3\%}$; $x_{11} = \frac{AI - 50^\circ}{10^\circ}$;

and $x_{12} = \frac{RS - 30\text{rpm}}{20\text{rpm}}$

The effect of operating conditions on $F_{C,max}$ was similar to that observed for the angle of departure and this result is

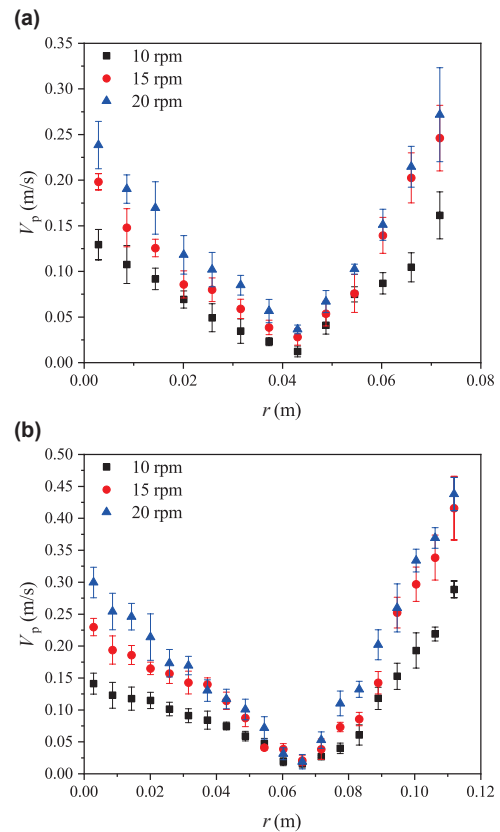


Fig. 9 Velocity profiles of glass beads for an angle of inclination of 50°: (a) 2 % and (b) 5 %.

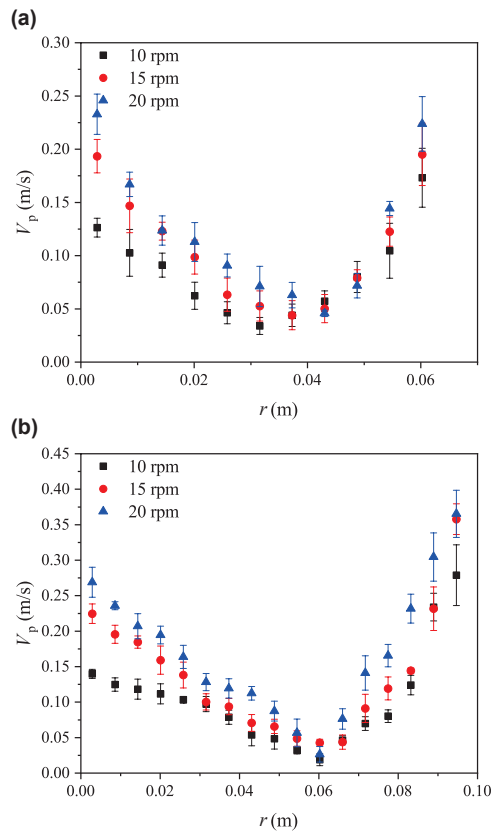


Fig. 10 Velocity profiles of glass beads for an angle of inclination of 60°: (a) 2 % and (b) 5 %.

in agreement with the behavior observed by Lima et al. (2022).

4.4 Simulation of particle velocity distributions

Due to the rotating disc inclination, the active and passive layers of the rolling regime were found to be located in the inner regions of the granular bed. Therefore, they could only be observed through simulations.

Figs. 9 and **10** display the particle velocity distributions, where V_p is the particle velocity and r is the particle position along the reference line (**Fig. 4(b)**). The variable r starts from the disc wall and ends at the granular bed surface. In this work, only the cases in which the rotating disc was operating in the rolling regime were considered, i.e., at angles of inclination of 50 (**Fig. 9**) and 60° (**Fig. 10**), filling degrees of 2 and 5 %, and velocities of 10, 15 and 20 rpm.

The two different bed structure regions visualized in the **Figs. 9** and **10** demonstrate that as the value of r increased, the particle velocities decreased until reaching a minimum value (close to zero), evidencing the interface between the passive and active layers. This behavior is typical of the passive layer in the rolling regime, in which the particles move as a solid body and are dragged up by the disc wall. From the interface, the solids velocities started to increase along r , characterizing the active layer. In this region, the

Table 8 Analysis of active and passive layer thicknesses.

Angle of inclination	Filling degree [%]	Layer thickness [m]		Ratio (A/P)
		Passive (P)	Active (A)	
50°	2	0.040	0.029	0.714
	5	0.063	0.046	0.727
60°	2	0.034	0.023	0.667
	5	0.057	0.034	0.600

particles had a higher dynamics, moving in the opposite direction to the passive layer. As observed, the highest velocity values were found to be near the granular bed surface.

It can also be seen that higher rotational speeds resulted in greater velocities in both layers, but without changing the interface position. When the rotational speed was kept constant and the filling degree was increased, the particle velocities also increased in both layers, and such effect was higher in the active layer. Regarding the angle of inclination, it can be observed that the disc operating at 50° achieved higher particle velocities in the active layer. In this case, the granular bed reached a higher angle of departure, increasing the potential energy of the particles and therefore their dynamics.

In contrast to the rotational speed, changes in the filling degree and angle of inclination modified the interface position, suggesting the significant impact of these variables on the active layer thickness. The correct prediction of the active and passive layers for a rotating disc operating in the rolling regime is very important for the granulation process. It is worth mentioning that the best particle interactions, mixing and segregation, as well as the highest rates of heat and mass transfer, occur in the active layer. **Table 8** presents the thicknesses of the active layers and their ratio to the passive layer thicknesses for angles of inclination of 50° and 60°.

For constant filling degrees, the change in the angle of inclination from 50° to 60° resulted in a reduced ratio between the layers of 6.58 % and 17.47 % for filling degrees of 2 % and 5 %, respectively, evidencing the movement of particles to the passive layer region.

Santos et al. (2015) found similar behavior, when studied, numerically and experimentally, the velocity profile of soybean particles in a rotating drum operating in the rolling regime. They observed that, keeping the filling degree constant and increasing the rotational speed, there was an increase in the velocity of the particles in both layers (passive and active), and the point where a reverse of the flow takes place was kept constant. On the other hand, when the rotational speed was kept constant and the filling degree was changed from 18.81 % to 31.40 %, the inflection point

changed from 4 cm to 5.5 cm, respectively.

5. Conclusions

In this work, DEM simulations were performed to study the influence of DEM parameters and operating conditions on particle dynamics in a rotating disc.

The methodology used herein allowed to analyze and quantify the effect of DEM parameters on the number of contacts between particles, an important variable in the granulation process. All DEM parameters had a significant influence on the analyzed response, with μ_{Spw} being the parameter with the greatest effect.

DEM simulations were also used to predict the behavior of flow regimes in a rotating disc. In these simulations, the input parameters obtained from the experimental procedure were used and successfully predicted the experimental behavior of all flow regimes.

With respect to the effects of the operating conditions of the rotating disc (i.e., filling degree, angle of inclination and rotational speed) on $N_{C_{pp}}$ and $F_{C,max}$, it was observed that the increase in the filling degree had a positive effect on both responses. In contrast, the increase in the rotational speed led to a reduction in $N_{C_{pp}}$, but an increase in $F_{C,max}$, which can impair the efficiency of the granulation process. Lastly, in relation to the disc inclination, the change in this parameter had little influence on $N_{C_{pp}}$. Additionally it was verified that greater angles of inclination led to a reduction in the intensity of $F_{C,max}$.

In this study, it is also possible to verify the effect of the operating conditions of the rotating disc on the particle velocity distributions in the rolling regime. As the filling degree and rotational speed increased, the particle velocity was also raised in both layers, whilst the change in the angle of inclination affected the active layer. The disc operating at 50° showed the highest ratio between the active and passive layer thicknesses.

Supplementary information

The online version contains supplementary material available at <https://doi.org/10.14356/kona.2024016>.

Acknowledgments

The authors are grateful to the Minas Gerais Research Funding Foundation (FAPEMIG), the Brazilian National Council for Scientific and Technological Development (CNPq), and the Coordination for the Improvement of Higher Education Personnel (CAPES) for their financial support.

Nomenclature

D	diameter of disc granulator (m)
D_r	distance traveled by the particle (m)
e	restitution coefficient (-)

E	Young's modulus (Pa)
E^*	equivalent Young's modulus (Pa)
F	force (N)
G	shear modulus (Pa)
G^*	equivalent shear modulus (Pa)
h_0	device height (m)
I	moment of inertia ($m^2 s^{-2}$)
L	rim height of disc granulator (m)
m^*	equivalent mass (kg)
m	mass (kg)
N_c	number of contact (-)
R	radius (m)
R^*	equivalent contact radius (m)
S	stiffness (Pa m)
t	time (s)
v	linear velocity (ms^{-1})
V_0	velocity before impact ($m s^{-1}$)
V_1	velocity after impact ($m s^{-1}$)
V_p	particle velocity ($m s^{-1}$)
Greek Symbol	
α	angle of departure (°)
β	damping coefficient ($kg s^{-1}$)
δ	overlap distance of two particles (m)
θ	angle of inclination of disc granulator (°)
μ_R	rolling friction coefficient (-)
μ_S	static friction coefficient (-)
τ	torque ($N m^{-1}$)
ν	Poisson ratio (-)
Φ	angle of inclination used in the friction coefficient measurement (-)
ω	angular velocity (s^{-1})
Indexes	
C	contact
d	damping
i and j	particle identification index
n	normal direction
pp	particle–particle interaction
pw	particle–wall interaction
t	tangential direction

References

- ASTM G115 - 10, Standard guide for measuring and reporting friction coefficients, American Society for Testing and Materials (ASTM), (2013). DOI: 10.1520/G0115-10R13.2
- Azrar H., Zentar R., Abriak N.E., The effect of granulation time of the pan granulation on the characteristics of the aggregates containing Dunkirk sediments, *Procedia Engineering*, 143 (2016) 10–17. DOI:

- 10.1016/j.proeng.2016.06.002
- Ball F.D., Pelletizing before sintering: some experiments with a disc, *Journal of the iron and steel institute*, 192 (1959) 40–55.
- Barrios G.K.P., de Carvalho R.M., Kwade A., Tavares L.M., Contact parameter estimation for DEM simulation of iron ore pellet handling, *Powder Technology*, 248 (2013) 84–93. DOI: 10.1016/j.powtec.2013.01.063
- Bharadwaj R., Ketterhagen W.R., Hancock B.C., Discrete element simulation study of a Freeman powder rheometer, *Chemical Engineering Science*, 65 (2010) 5747–5756. DOI: 10.1016/j.ces.2010.04.002
- Brandao R.J., Lima R.M., Santos R.L., Duarte C.R., Barrozo M.A.S., Experimental study and DEM analysis of granular segregation in a rotating drum, *Powder Technology*, 364 (2020) 1–12. DOI: 10.1016/j.powtec.2020.01.036
- Capes C.E., *Particle Size Enlargement*, 1st ed, Elsevier, Elsevier, Amsterdam, 1980, ISBN: 9781483275079.
- Chadwick P.C., Bridgwater J., Solids flow in dish granulators, *Chemical Engineering Science*, 52 (1997) 2497–2509. DOI: 10.1016/S0009-2509(97)00068-7
- Cundall P.A., Strack O.D.L., A discrete numerical model for granular assemblies, *Géotechnique*, 29 (1979) 47–65. DOI: 10.1680/geot.1979.29.1.47
- Cunha R.N., Santos K.G., Lima R.N., Duarte C.R., Barrozo M.A.S., Repose angle of monparticles and binary mixture: an experimental and simulation study, *Powder Technology*, 303 (2016) 203–211. DOI: 10.1016/j.powtec.2016.09.023
- Delele M.A., Weigler F., Franke G., Mellmann J., Studying the solids and fluid flow behavior in rotary drums based on a multiphase CFD model, *Powder Technology*, 292 (2016) 260–271. DOI: 10.1016/j.powtec.2016.01.026
- Di Maio F.P., Di Renzo A., Modelling particle contacts in distinct element simulations: linear and non-linear approach, *Chemical Engineering Research and Design*, 83 (2005) 1287–1297. DOI: 10.1205/cherd.05089
- El Kassem B., Salloum N., Brinz T., Heider Y., Markert B., A semi-automated dem parameter calibration technique of powders based on different bulk responses extracted from auger dosing experiments, *KONA Powder and Particle Journal*, 38 (2021) 235–250. DOI: 10.14356/kona.2021010
- Gladky A., Lieberwirth H., Lampke J., Schwarze R., Numerical modeling of bulk flow on a pelletizing disc in different rotational regimes, *Granular Matter*, 23 (2021) 1–9. DOI: 10.1007/s10035-021-01121-6
- Hastie D.B., Experimental measurement of the coefficient of restitution of irregular shaped particles impacting on horizontal surfaces, *Chemical Engineering Science*, 101 (2013) 828–836. DOI: 10.1016/j.ces.2013.07.010
- Lima R.M., Brandao R.J., Santos R.L., Duarte C.R., Barrozo M.A.S., Analysis of methodologies for determination of DEM input parameters, *Brazilian Journal of Chemical Engineering*, 38 (2021) 287–296. DOI: 10.1007/s43153-021-00107-4
- Lima R.M., Brandão R.J., Souza G.M. De, Silveira J.C., Potenza F., Duarte C.R., Barrozo M.A.S., Analysis of particle dynamics in a rotating dish, *Powder Technology*, 409 (2022) 117827. DOI: 10.1016/j.powtec.2022.117827
- Litster J., Ennis B., *The Science and Engineering of Granulation Processes*, Springer Netherlands, Dordrecht, 2004, ISBN: 9781402018770. DOI: 10.1007/978-94-017-0546-2
- Machado M.V.C., Santos D.A., Barrozo M.A.S., Duarte C.R., Experimental and numerical study of grinding media flow in a mill, *Chemical Engineering and Technology*, 40 (2017) 1835–1843. DOI: 10.1002/ceat.201600508
- Marigo M., Stitt E.H., Discrete element method (DEM) for industrial applications: comments on calibration and validation for the modelling of cylindrical pellets, *KONA Powder and Particle Journal*, 32 (2015) 236–252. DOI: 10.14356/kona.2015016
- Marinack Jr. M.C., Musgrave R.E., Higgs C.F., Experimental investigations on the coefficient of restitution of single particles, *Tribology Transactions*, 56 (2013) 572–580. DOI: 10.1080/10402004.2012.748233
- Mellmann J., The transverse motion of solids in rotating cylinders-forms of motion and transition behavior, *Powder Technology*, 118 (2001) 251–270. DOI: 10.1016/S0032-5910(00)00402-2
- Nascimento S.M., Lima R.M., Brandão R.J., Santos D.A., Duarte C.R., Barrozo M.A.S., Comparison between the Eulerian (CFD) and the Lagrangian (DEM) approaches in the simulation of a flighted rotary drum, *Computational Particle Mechanics*, 9 (2022) 251–263. DOI: 10.1007/s40571-021-00407-z
- O’Sullivan C., *Particulate Discrete Element Modelling*, Particulate Discrete Element Modelling, CRC Press, London, 2011, ISBN: 9780429077517. DOI: 10.1201/9781482266498
- Pietsch W., Size Enlargement by Agglomeration, in: Fayed M.E., Otten L.(eds.), *Handbook of Powder Science & Technology*, Springer New York, 1997, pp. 202–377 ISBN: 9780412996214. DOI: 10.1007/978-1-4615-6373-0
- Potyondy D.O., Cundall P.A., A bonded-particle model for rock, *International Journal of Rock Mechanics and Mining Sciences*, 41 (2004) 1329–1364. DOI: 10.1016/j.ijrmms.2004.09.011
- Resende I.A., Machado M.V.C., Duarte C.R., Barrozo M.A.S., An experimental analysis of coffee beans dynamics in a rotary drum, *Canadian Journal of Chemical Engineering*, 95 (2017) 2239–2248. DOI: 10.1002/cjce.22961
- Rong W., Feng Y., Schwarz P., Yurata T., Witt P., Li B., Song T., Zhou J., Sensitivity analysis of particle contact parameters for DEM simulation in a rotating drum using response surface methodology, *Powder Technology*, 362 (2020) 604–614. DOI: 10.1016/j.powtec.2019.12.004
- Salman A.D., Hounslow M.J., Seville J.P.K., *Granulation*, Handbook of Powder Technology, 1st edition, Elsevier Science, 2006, ISBN: 9780080467887.
- Santos D.A., Barrozo M.A.S., Duarte C.R., Weigler F., Mellmann J., Investigation of particle dynamics in a rotary drum by means of experiments and numerical simulations using DEM, *Advanced Powder Technology*, 27 (2016) 692–703. DOI: 10.1016/j.appt.2016.02.027
- Santos D.A., Dadalto F.O., Scatena R., Duarte C.R., Barrozo M.A.S., A hydrodynamic analysis of a rotating drum operating in the rolling regime, *Chemical Engineering Research and Design*, 94 (2015) 204–212. DOI: 10.1016/j.cherd.2014.07.028
- Santos D.A., Petri I.J., Duarte C.R., Barrozo M.A.S., Experimental and CFD study of the hydrodynamic behavior in a rotating drum, *Powder Technology*, 250 (2013) 52–62. DOI: 10.1016/j.powtec.2013.10.003
- Tsuji Y., Tanaka T., Ishida T., Lagrangian numerical simulation of plug flow of cohesionless particles in a horizontal pipe, *Powder Technology*, 71 (1992) 239–250. DOI: 10.1016/0032-5910(92)88030-L

Authors' Short Biographies



Rondinelli Moulin Lima

Dr. Rondinelli Moulin Lima received his Ph. D. in Chemical Engineering from the Federal University of Uberlândia in 2021. He has experience in Chemical Engineering, with emphasis on Computational Fluid Dynamics and Discrete Element Method in the area of particulate systems and separation processes. He is currently a researcher at the Institutional Training Program at the Center for Mineral Technology (CETEM), with the development of agglomerated stones.



Gisele Márcia de Souza

MSc. Gisele Márcia de Souza received her master's degree in Metallurgical and Mining Engineering from the Federal University of Minas Gerais. Currently, she is a Ph. D. candidate at the Federal University of Uberlândia in the area of particulate systems and separation processes. She has experience in Chemical Engineering, with emphasis on Transport Phenomena, Unit Operations, Computational Fluid Dynamics and Discrete Element Method.



Rodolfo Junqueira Brandão

Dr. Rodolfo Junqueira Brandão is Adjunct Professor I at the Technology Center at the Federal University of Alagoas. He received his Ph. D. in Chemical Engineering from the Federal University of Uberlândia in 2019. He is currently Coordinator of the Technology Center and Tutor of the Special Engineering Training Program. He works mainly in the area of particulate systems, separation processes and numerical simulation.



Claudio Roberto Duarte

Dr. Claudio Roberto Duarte is a Full Professor at the Federal University of Uberlândia in Brazil. He received his Ph. D. in Chemical Engineering from the Federal University of Uberlândia in 2006. He served as the Coordinator of the Postgraduate Program in Chemical Engineering at the Federal University of Uberlândia from 2019 to 2022. He works mainly on the following topics: granulation, rotating drums, mills, drying, pyrolysis, solid-liquid separation, spouted bed, modelling, computational fluid dynamics, and cyclone.



Marcos Antonio de Souza Barrozo

Dr. Marcos Antonio de Souza Barrozo is a Full Professor at the Federal University of Uberlândia in Brazil. He received his Ph. D. in Chemical Engineering from the Federal University of São Carlos in 1995. He is an A1 researcher at the National Council for Scientific and Technological Development (CNPq) and a member of the Standing Committee of the Brazilian Congress of Particulate Systems. He has experience in Particulate Systems, working mainly on the following topics: fluid dynamics of particulate systems, solid-fluid separation, drying, coating, granulation, flotation, pyrolysis, and hydrothermal carbonization.